

Macrophage-derived exosomes accelerate wound healing through their anti-inflammation effects in a diabetic rat model

Mengdie Li, Tao Wang, He Tian, Guohua Wei, Liang Zhao & Yijie Shi

To cite this article: Mengdie Li, Tao Wang, He Tian, Guohua Wei, Liang Zhao & Yijie Shi (2019) Macrophage-derived exosomes accelerate wound healing through their anti-inflammation effects in a diabetic rat model, *Artificial Cells, Nanomedicine, and Biotechnology*, 47:1, 3793-3803, DOI: [10.1080/21691401.2019.1669617](https://doi.org/10.1080/21691401.2019.1669617)

To link to this article: <https://doi.org/10.1080/21691401.2019.1669617>



© 2019 The Author(s). Published by Informa UK Limited, trading as Taylor & Francis Group



View supplementary material [↗](#)



Published online: 26 Sep 2019.



Submit your article to this journal [↗](#)



Article views: 4269



View related articles [↗](#)



View Crossmark data [↗](#)



Citing articles: 37 View citing articles [↗](#)

Macrophage-derived exosomes accelerate wound healing through their anti-inflammation effects in a diabetic rat model

Mengdie Li^{a*}, Tao Wang^{a*}, He Tian^{b*}, Guohua Wei^c, Liang Zhao^a and Yijie Shi^a

^aSchool of Pharmacy, Jinzhou Medical University, Jinzhou, P R China; ^bDepartment of Histology and Embryology, Jinzhou Medical University, Jinzhou, P R China; ^cDepartment of Pathology, The First Affiliated Hospital of Jinzhou Medical University, Jinzhou, P R China

ABSTRACT

Chronic, subclinical inflammation was often observed in the diabetic wound area, causing inadequate and delayed wound-healing effects by failing to initiate cell migration, proliferation, and extracellular matrix deposition. Therefore, we presented macrophage-derived exosomes (Exos) and explored their potential for inhibiting inflammation and accelerating diabetic wound healing in a skin defect, diabetic rat model. A thorough investigation demonstrated that Exos exerted anti-inflammatory effects by inhibiting the secretion of pro-inflammatory enzymes and cytokines. Furthermore, they accelerated the wound-healing process by inducing endothelial cell proliferation and migration to improve angiogenesis and re-epithelialization in diabetic wounds.

ARTICLE HISTORY

Received 31 May 2019
Revised 24 August 2019
Accepted 24 August 2019

KEYWORDS

Diabetes; inflammation; wound healing; exosomes; angiogenesis

Introduction

Diabetic wound dysfunction is a serious, chronic complication of diabetes. Nearly 15% of 150 million diabetic patients worldwide suffer diabetic wound injury, which accounts for 50% of cases necessitating amputation treatment [1,2]. Given its high incidence of morbidity and mortality, diabetic wound damage brings a heavy burden to patients and society. Therefore, determining the pathogenesis and enhancing therapeutic efficacy of diabetic wound disease have become a main focus in diabetes research.

Diabetic chronic wounds, characterized by a persistent inflammatory response, exhibit a pathologically delayed healing process by altering angiogenesis, ultimately delaying epithelialization and inducing imbalanced secretion in protease [3].

With the extension of the inflammatory phase in the diabetic wound-healing process, inflammatory cells were generally activated, thus delaying the switch from inflammatory phase to proliferative phase [4]. A large amount of inflammatory mediators, such as tumor necrosis factor (TNF)- α and interleukin (IL)-6, secreted by cells were released into the wound site and subsequently prevented the cell proliferation and migration required for diabetic wound healing [5]. Furthermore, over-activation of inflammation increased matrix metalloproteinase (MMP)-9 expression [6,7], which resulted in rapid degradation of native collagen, fibronectin, and elastin, thus delaying the diabetic wound-healing process [8].


Exosomes are bilayer nanovesicles secreted by most embryonic cells and take charge of cell-to-cell communication by delivering lipids, proteins, and nucleic acids to neighboring cells [9–12]. Given their low malignant potential, cellular/tissue specificity and potent immunomodulatory effects, exosomes have been widely applied to accelerate wound healing and demonstrated promising results [13–15].

Increasing data indicate that macrophages may create an optimal microenvironment for reducing inflammation through a paracrine mechanism [16–18], and exosomes secreted by macrophages play an important role in communicating with neighboring cells via regulating levels of cytokines and miRNAs to ameliorate the inflammatory response in recipient cells [19,20]. It has been reported that macrophage-derived exosomes attenuated thermal hyperalgesia in a murine model of inflammatory pain, suggesting their role in dysregulated inflammation [21].

In this study, we hypothesized that exosomes derived from macrophages (Exos) can prevent inflammatory activation at the diabetic wound site, which contribute to rapid diabetic wound healing. We observed that macrophage-derived exosomes significantly attenuated the secretion of pro-inflammatory cytokine and promoted proliferation and migration of endothelial cells to improve angiogenesis and re-epithelialization in diabetic wounds. It demonstrated that given their heightened anti-inflammatory potential, Exos are a promising approach for accelerating diabetic wound healing in future clinical applications.

CONTACT Liang Zhao  liangzhao79@163.com; Yijie Shi  shiyijie119@163.com  School of Pharmacy, Jinzhou Medical University, Jinzhou, 121000, P R China

*These three authors contributed equally to the manuscript

 Supplemental data for this article is available online at <https://doi.org/10.1080/21691401.2019.1669617>.

© 2019 The Author(s). Published by Informa UK Limited, trading as Taylor & Francis Group
This is an Open Access article distributed under the terms of the Creative Commons Attribution License (<http://creativecommons.org/licenses/by/4.0/>), which permits unrestricted use, distribution, and reproduction in any medium, provided the original work is properly cited.

Materials and methods

Cells and cell culture

RAW 264.7 cells (ATCC® TIB-71™; American Type Culture Collection [ATCC], Manassas, VA, USA) were purchased from the Cell Bank of the Chinese Academy of Sciences (Shanghai, China). RAW 264.7 cells (ATCC® TIB-71™) were maintained in complete media ($1 \times$ DMEM, 10% heat-inactivated fetal bovine serum [FBS]). Human umbilical vein endothelial cells (HUVECs, Cell Bank of the Chinese Academy of Sciences, Shanghai, China) were cultured in F12 medium (Gibco BRL) containing 10% FBS (Gibco BRL). In order to mimic diabetic environment *in vitro*, high glucose cultured HUVECs (HG-HUVECs) had confirmed to be often employed and obtained by using high glucose (HG;40 mM) to treat HUVECs for 72 h (the media were changed every 24 h), as previously described [22,23]. To further explore Exos-induced anti-inflammation effects in the cells, lipopolysaccharide (LPS) was used as an activator of the inflammatory response to induce enhanced inflammation and combined with Exos to treat cells [24].

Preparation and purification of macrophage-derived exosomes

For exosomes collection, RAW 264.7 cells (1×10^7) were plated in 150 mm dishes with complete culture media. After 24 h of culturing, the media was replaced with exosome-depleted media ($1 \times$ DMEM, 10% heat-inactivated FBS depleted of exosomes by ultracentrifugation). The cell culture medium was collected and centrifuged at 15,000 rpm for 30 min to remove cell debris and macromolecular proteins, which was followed by filtration through a 0.22 μ m filter. Finally, after centrifugation with an ultracentrifuge at 57,000 rpm for 1 h, the supernatant was removed and the transparent precipitate from the bottom of the centrifuge tube was collected to obtain macrophage-derived exosomes (Exos). The morphology and shape of Exos were determined by means of transmission electron microscope (JEM-1200EX; JEOL, Tokyo, Japan). Particle size and surface charge of the exosomes were measured using Zetasizer Nano ZS (Malvern Instruments, Malvern, UK). To explore the identification of Exos, western blot assay was performed to detect CD63 and Alix (known as exosomal markers), which were enriched in the exosome pellet fraction.

Cell proliferation determination

The effects of Exos on the proliferation of HG-HUVECs were investigated using a cell viability assay (Cell Counting Kit-8 [CKK-8]; Dojindo Molecular Technologies, Inc., Kumamoto, Japan). HG-HUVECs at a density of 5×10^4 /mL were seeded into the 96-well plate (100 μ L each well) and incubated for 24 h at 37 °C under 5% CO₂. The medium was replaced by serum-free medium in the presence of low Exos concentrations (Exos low, 50 μ g/mL), high Exos concentrations (Exos high, 500 μ g/mL), and the combination of Exos at 500 μ g/mL and LPS at 100 ng/mL (Exos high + LPS), respectively. After 48 h, 20 μ L of CCK-8 solution and 180 μ L of fresh culture

medium were added to each well at each time point and incubated for 1 h at 37 °C. Then, the absorbance was measured at 450 nm using a microplate reader (Synergy-2; BioTek, Winooski, VT, USA). All experiments were performed thrice.

Tube formation assay

A total of 200 μ L of matrigel was pipetted into each well of a 24-well plate and incubated at 37 °C and 5% CO₂ for 30 min to solidify. HG-HUVECs (80 μ L/well, approximately 1×10^5 cells/well) were seeded into each well loaded with matrigel on the bottom, followed by the addition of Exos, and they were continuously incubated for 8 h. The total branching points and total tube length of HG-HUVECs were observed and analyzed using a confocal microscope (Leica DMI6000B; Leica Microsystems, Wetzlar, Germany) and imaged at 100 \times magnification.

Scratch wound assay

For the scratch wound assay, HG-HUVECs were cultured in F12 and DMEM supplemented with 10% FBS and seeded into a 24-well tissue culture plate until they reached 100% confluence as a monolayer. A new 200 μ L pipette tip was used to gently and slowly scratch a straight line into the monolayer across the center of the well. After scratching, wells were washed twice with medium to remove the detached cells, followed by replenishing the wells with fresh medium. The different concentrations of Exos were added into the wells and co-incubated with cells at 37 °C. At different time intervals, the cells were washed twice with PBS, and the gap distance was observed and quantitatively evaluated under the microscope.

Transwell assay

HG-HUVECs in logarithmic growth phase were trypsinized and seeded into the transwell insert precoated with basement membrane matrigel followed by the addition of Exos. Complete medium (containing 10% FBS) was placed in the lower chamber. After 12 h, cells were fixed by submerging the insert in 4% paraformaldehyde for 20 min and stained with 1% crystal violet for 30 min. Cells were removed from the unmigrated (top) side by gently scraping this side with a wet Q-tip/cotton swab. Migration was determined by counting cells on the lower surface of the filter and the level of migration was observed under an optical microscope (Leica DMI6000B; Leica Microsystems).

Establishment of diabetic rat wound models and treatment

All procedures were approved by the Animal Research Committee of Jinzhou Medical University. Streptozotocin (STZ; Sigma-Aldrich Co., St. Louis, MO, USA) was injected into Sprague–Dawley (SD) rats intraperitoneally at a dosage of 100 mg/kg/body weight once per day for 4 consecutive days until the animals' blood glucose levels were >300 mg/dL.

This proved that a hyperglycemic phenotype was formed, and that type 1 diabetes was induced in the SD rats. The rats were anesthetized with 2% isoflurane and round, full-thickness excision skin wounds with a diameter of 1.5 cm were produced on the backs of the rats. On the day when the wounds were produced (day 0), the diabetic wound sites were treated with 1 ml PBS, 1 ml of low-concentration Exos (100 µg/mL), high-concentration Exos (1 mg/mL) and the combination of high-concentration Exos (1 mg/mL) and LPS (10 µg/mL), respectively, per wound by subcutaneous injection. Wound area-reducing curves were determined by calculating the ratio of the initial wound area to the wound area at different times. The reduction of wound size was calculated using the following mathematical equation:

$$\text{Wound size reduction (\%)} = (A_0 - A_t) / A_0 \times 100\% \quad (1)$$

Where A_0 is the initial wound area and A_t is the wound area at days 7, 14, and 21 post-operation. On days 7 and 14, the muscle and skin around the wound were excised and fixed in 10% buffered formalin. The tissue was embedded in paraffin and sectioned vertically at 5 µm for staining.

H&E staining

Paraffin sections of skin were dewaxed in water; then, the sections were incubated with hematoxylin for 5 min. After hydrochloric acid color separation for 2 s, the sections were rinsed (using running water) for 30 min. Next, the sections were incubated with eosin for 3 min. After several rinses, the sections were dehydrated in gradient alcohol, transparented with xylene, and sealed using neutral gum. Images were collected under a microscope and quantified using Image-Pro Plus 6.0 analysis software.

Masson's trichrome staining

Masson's trichrome assay was applied to evaluate the degree of collagen maturity. Sections were deparaffinized and rehydrated. Masson staining was performed according to the manufacturer's instructions. Images were collected under a microscope and quantified using Image-Pro Plus 6.0 analysis software.

Immunohistochemistry staining and immunofluorescence staining analysis

Sections were dewaxed in xylene and rehydrated using gradient alcohol solutions. Then, the sections were treated with 3% hydrogen peroxide (H_2O_2) for 10 min, and antigen retrieval was performed by incubation in citrate buffer (pH 6.0) at high pressure for 3 min. After rinsing with PBS, the sections were blocked with goat serum for 20 min for immunohistochemistry staining and immunofluorescence staining analysis.

Statistical analysis

All data are presented as the means \pm standard deviations (SD). Independent-samples t -tests were used to compare the means between two different groups. One-way analysis of variance (ANOVA) was used to determine the level of significance with GraphPad Prism software (GraphPad, La Jolla, CA, USA), and p values $< .05$ were considered statistically significant.

Results

Characterization of exos

RAW 264.7 cells were cultured and then Exos were isolated from the culture supernatants of RAW 264.7 cells by ultracentrifugation. Typical exosomal structures were observed by TEM and characterized as homogeneous and spherical vesicles, with a mean particle diameter of 95 ± 9.9 nm for Exos (Figure 1). Western blot analysis showed that CD63 and Alix (known exosomal markers) were enriched in the Exos pellet fraction, whereas they were not obviously detected in the supernatant, indicating that Exos had been fully collected from the culture medium.

Exos improved angiogenesis in HG-HUVECs in vitro

As angiogenesis is a vital process for skin wound healing and contributes to the formation and remodeling of new blood vessels, we investigated whether Exos could influence the angiogenic responses in HG-HUVECs. It was found that as shown in Figure 2(A–C), when compared to untreated HG-HUVECs as the control, Exos at low

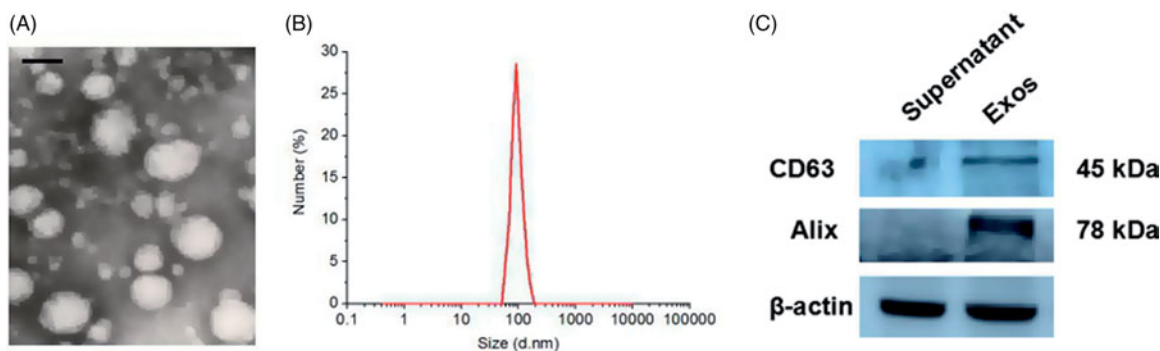


Figure 1. Characterization of Exos: (A) Morphology of Exos observed by TEM. The scale bar is 100 nm. (B) Particle size and distribution analysis of Exos. (C) Western blotting of Exos surface markers.

concentration of 50 $\mu\text{g/mL}$ and high concentration of 500 $\mu\text{g/mL}$ significantly increased the number of migrating cells and reduced the scratched area in a dose-dependent manner. The growth of Exos-treated HG-HUVECs, as measured by the CCK8 assay, had been significantly increased and their proliferation rates were enhanced by 1.9-fold and 2.8-fold for the group treated with Exos at low and high concentrations as compared to the control, respectively, within 48 h (Figure 2(D)). Matrigel tube formation results (Figure 2(B,C)) also demonstrated that when compared to the control group, tube formation in the presence of Exos was significantly accelerated, and the branch numbers of connected cells and the numbers of tubes formed in

randomly selected fields were significantly increased. Lipopolysaccharides (LPS) as an activator of the inflammatory response to induce inflammation [25], was combined with Exos to treat HG-HUVECs for investigating the inflammation-induced angiogenic response. After being treated with a combination of Exos at 500 $\mu\text{g/mL}$ and LPS at 100 ng/mL, cell proliferation, the number of migrated cells, and tube formation were significantly decreased and the scratched area was bigger as compared to that of Exos alone at 500 $\mu\text{g/mL}$ ($p < .05$). All these data demonstrated that Exos contributed to promotion of HG-HUVECs migration and tube formation and the addition of LPS abolished Exos-induced angiogenesis.

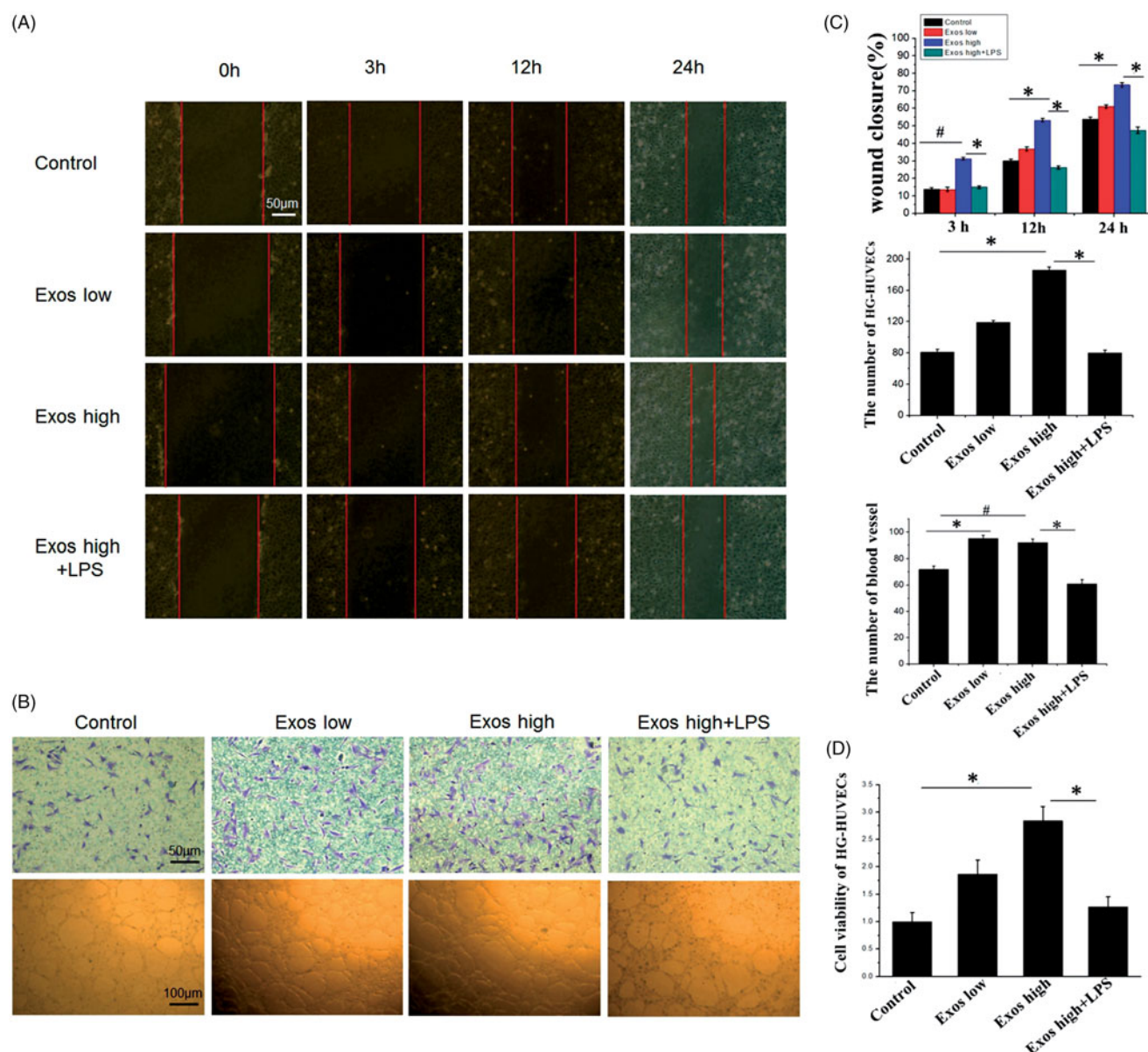


Figure 2. When low Exos concentrations (50 $\mu\text{g/mL}$) (Exos low) and high Exos concentrations (500 $\mu\text{g/mL}$) (Exos high) and the combination of high Exos (500 $\mu\text{g/mL}$) and LPS (100 ng/mL) concentrations (Exos high + LPS) were used to treat HG-HUVECs, Exos induced pro-angiogenic effects. untreated HG-HUVECs was used as the control group. (A) Exospromoted HG-HUVEC migration, as analyzed by scratch wound assay; this effect was reduced by Exos + LPS. (B) The migrating images of HG-HUVECs receiving different treatments were further confirmed by the transwell assay. Representative images of HG-HUVEC tube formation in different treatment groups. (C) Quantitative analysis of the scratch wound assay, transwell assay, and the tube-formation assay. The data are represented as the means \pm SD ($n = 3$), # $p < .05$, compared untreated HG-HUVECs (control) with high Exos levels (500 $\mu\text{g/mL}$). * $p < .05$. (D) Cell viability was analyzed by CCK-8 assay with different treatments. The data are represented as the means \pm SD ($n = 3$), * $p < .05$.

Exos promoted cell migration and proliferation in HG-HUVECs via anti-inflammation

In order to further confirm Exos-induced angiogenesis and proliferation via inhibiting the inflammatory response, some angiogenesis related proteins and inflammatory factors were determined by western blot. As shown in Figure 3, when compared to untreated HG-HUVECs as the control, Exos at low concentration of 50 $\mu\text{g/mL}$ and high concentration of 500 $\mu\text{g/mL}$ significantly decreased the expression of some inflammatory factors, such as tumor necrosis factor (TNF)- α , interleukin (IL)-6, indicating that Exos induced anti-inflammatory effects in HG-HUVECs. Furthermore, Exos also significantly enhanced the expression phosphorylated AKT and vascular endothelial growth (VEGF), indicating that AKT/VEGF signaling was activated in HG-HUVECs. Compared with Exos alone, the combination of Exos and LPS strengthened the inflammation by increasing TNF- α production from HG-HUVECs and counteracted Exos induced enhanced expression levels of AKT phosphorylation and VEGF. All western blot results revealed that Exos promoted angiogenesis in HG-HUVECs by inhibiting inflammation.

Evaluation of wound healing treated with Exos in type 1 diabetic rats

The wound-healing role of Exos in diabetic wounds was investigated by calculating the ratio of the initial wound area and the wound area at different times. As shown in Figure 4(A,C), when compared with the phosphate buffered saline (PBS) group, diabetic wound size reduction rate was enhanced by the application of Exos; thus the wound size

reduction were 18% for PBS, 64% for Exos at a low concentration of 100 $\mu\text{g/mL}$, and 81% for Exos at high a concentration of 1 mg/mL within 7 days. On day 14, the wounds were completely healed after being treated by Exos either at low or at high concentrations; the wound size reduction in both groups were over 94%. However, the wounds treated with PBS were still closing and had not yet been covered by new skin after 21 days, and the wound size reduction were 80% and 85% on the 14th and 21st day, respectively. The obtained results had fully validated the idea that Exos contributed to the wound-healing process by enhancing the wound size reduction. To determine whether Exos-mediated wound healing was related to regulation of the inflammatory process at the diabetic wound site *in vivo*, a combination of Exos at 1 mg/mL and LPS at 10 $\mu\text{g/mL}$ was applied to treat the wound via subcutaneous injection. It was found that LPS induced the inflammatory response at the wound site and actually reduced the wound-healing effects generated by Exos. The wound size reduction for the combination of Exos and LPS had been significantly reduced to 63% on day 7, and to 85% on day 14.

Light micrographs of hematoxylin and eosin (H&E)-stained sections indicated the level of wound contraction, which was defined as the length of the wound treated with PBS, Exos, and the combination of Exos and LPS. The equation below was used to calculate the wound contraction rate (E%): $E\% = L_N/L_O \times 100\%$. In the equation, L_O indicates the primitive wound length and L_N indicates the length of new epithelium [26]. As shown in Figure 4(B,D)), after 7 days, the Exos group significantly accelerated wound contraction over the wound-edge distance in the diabetic wound and the length of the wound was significantly reduced in the presence of Exos at

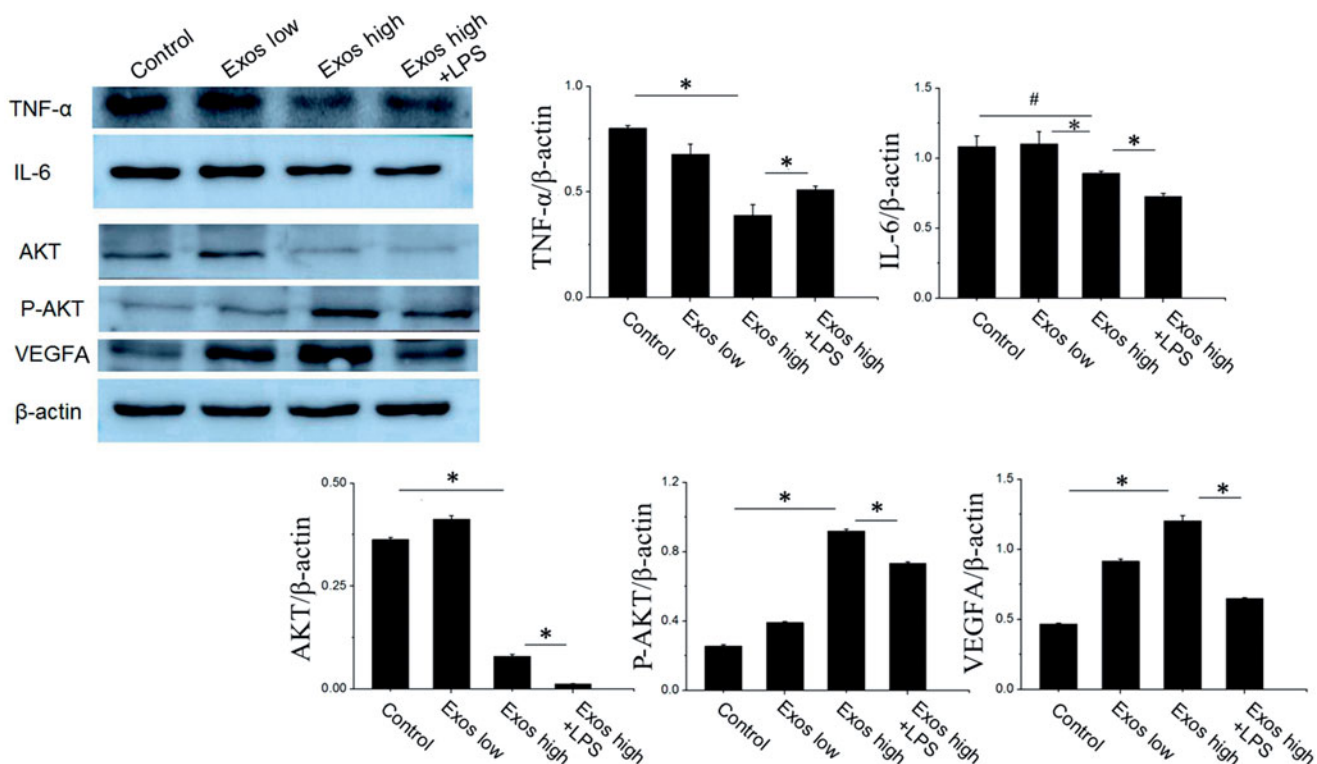


Figure 3. Detection of TNF- α , IL-6, AKT, P-AKT, and VEGF levels by Western blotting. The data are represented as the means \pm SD ($n = 3$), $\#p < .05$, compared untreated HG-HUVECs (control) with high Exos levels (500 $\mu\text{g/mL}$). $*p < .05$.

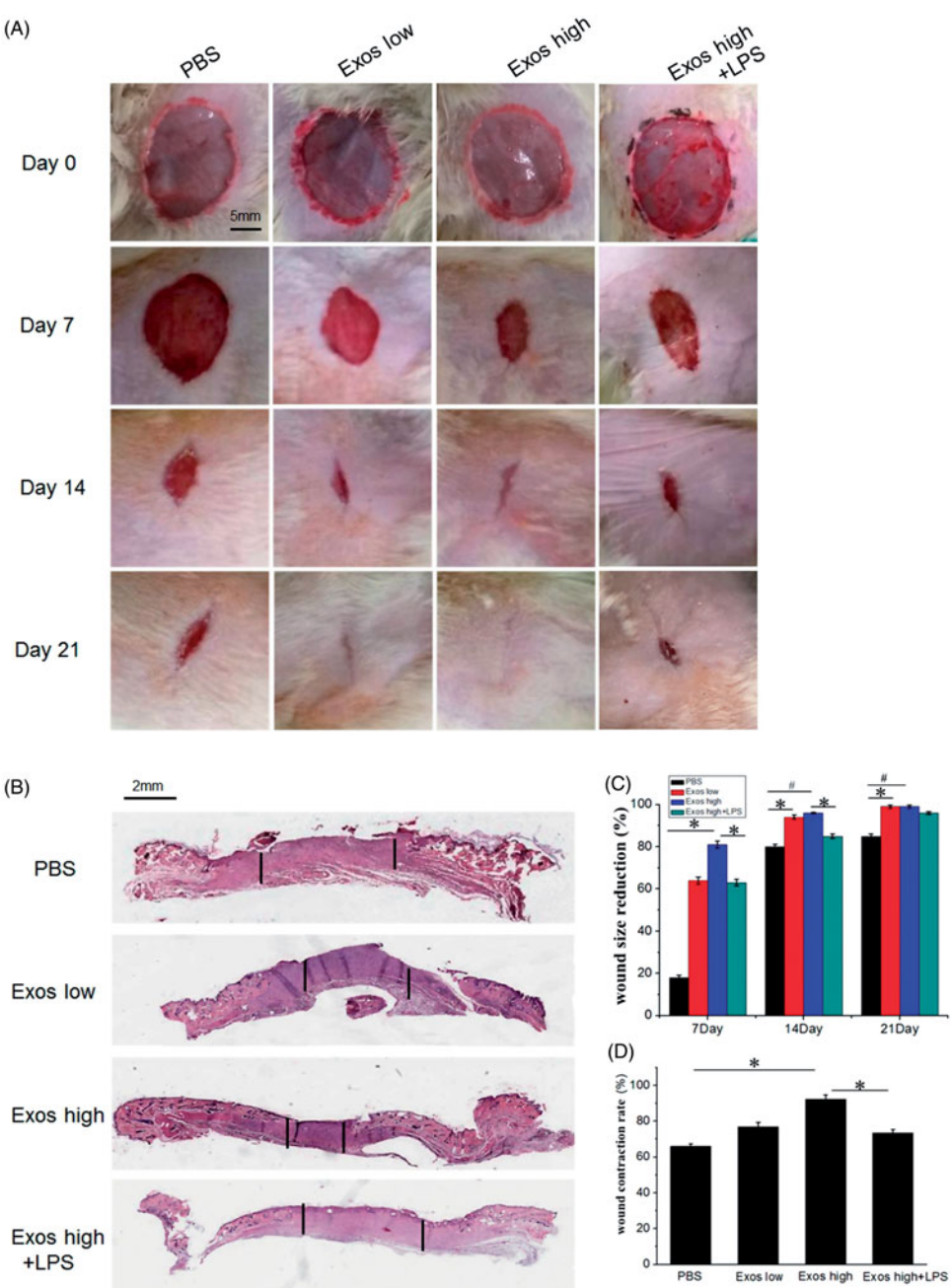


Figure 4. (A) Representative images of full-thickness skin defects in a diabetic rat model untreated (PBS) or treated with low Exos (100 µg/mL), high Exos (1 mg/mL), or high Exos (1 mg/mL) + LPS (10 µg/mL) at 0 days, 7 days, 14 days, and 21 days after operation. The scale bar in all Figure 4(A) is 5 mm. (B) Transmitted light images of H&E-stained sections of the untreated defects (PBS) and defects treated with low Exos, high Exos, or high Exos + LPS at day 7 after operation. (C) The wound size reduction in wounds receiving different treatments based on representative images of full-thickness skin defects in a diabetic rat model. The data are represented as the means ± SD ($n = 3$), # $p < .05$, compared PBS group with high Exos levels (1 mg/mL), * $p < .05$. (D) Determination of wound contraction rate based on transmitted light images of H&E-stained sections. The data are represented as the means ± SD ($n = 3$), * $p < .05$.

high concentrations of (1 mg/mL), particularly when compared with the PBS control. The presence of LPS significantly reduced the wound contraction rate, and the wound length treated with the combination of Exos and LPS was longer than that of the wound treated with Exos alone at day 7.

H&E staining analysis

To assess the healing effects of Exos at the diabetic wound site on SD rats, histopathological alterations in the wound were evaluated by H&E staining. Histological observations

(Figure 5) revealed that after 7 days of treatment, Exos significantly reduced the number of infiltrating inflammatory cells including neutrophils and macrophages when compared to the PBS control in diabetic wounds. After 14 days, a great number of inflammatory cells were still observed in the PBS control, while there was no obvious inflammatory infiltration found in diabetic wounds treated with Exos. It indicated that Exos significantly inhibited chronic inflammation in diabetic wound. Meanwhile, the Exos group promoted the formation of granulation tissue at the wound site, which featured increasing numbers of new blood vessels found within 7 days. Of note, the combination of Exos and LPS enhanced

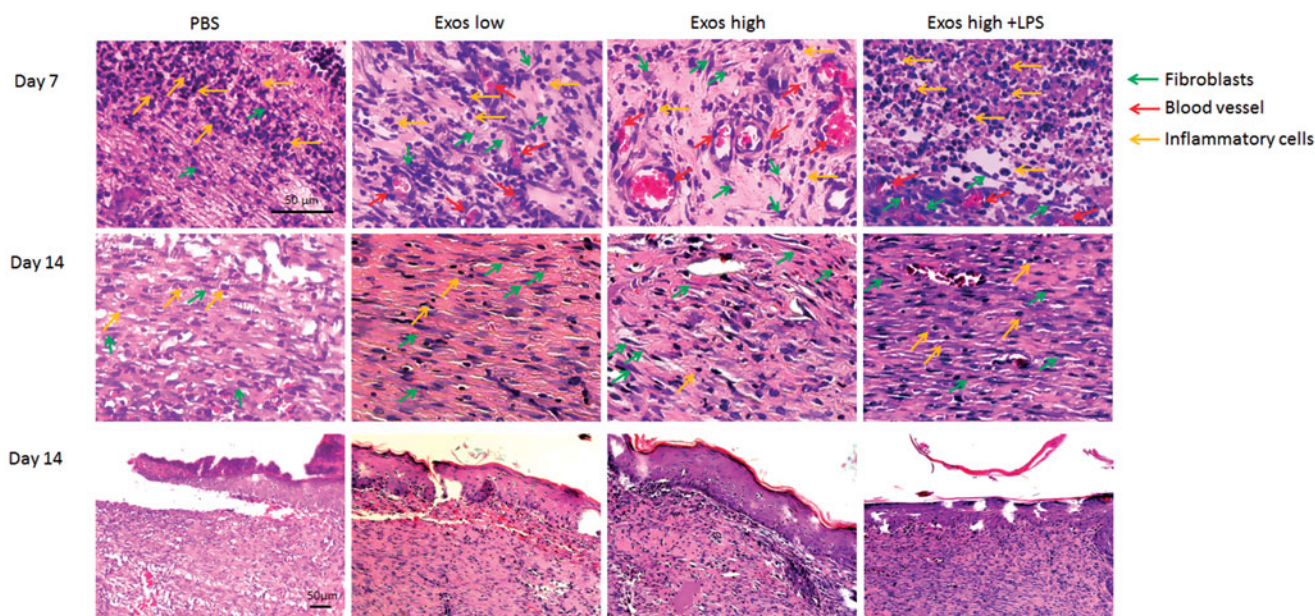


Figure 5. H&E staining of tissue sections treated with PBS, low Exos concentrations (100 µg/mL), high Exos concentrations (1 mg/mL), or high Exos (1 mg/mL) + LPS (10 µg/mL) concentrations on days 7 and 14. The scale bar in figure is 50 µm.

the infiltration of inflammatory cells and decreased the formation of new blood vessels, suggesting that LPS-induced local inflammation weakened the Exos-mediated wound-healing effects.

Masson staining analysis

The effect of Exos on wound extracellular matrix (ECM) production was analyzed by masson staining, and the results in Figure 6 showed that when compared with PBS as the control group, organized and dense collagen were deposited and a large number of sparse and scattered collagen fibers were found in the wounds treated with Exos. On the contrary, the combination of Exos and LPS exacerbated the local inflammation, thus reducing the production of collagen when compared with the treatment of Exos alone. Therefore, the results demonstrated that Exos treatments enhanced the collagen deposition and re-epithelialization for further accelerating wound healing.

Exos enhanced angiogenesis at the wound sites of SD rats with type 1 diabetes

We then asked whether the transplantation of Exos could enhance angiogenesis in the wound area. To evaluate the effects of Exos on the generation of newly formed blood vessels in the dermal defect, CD31 as an important indicator of neovascularization was stained for reflecting the formation of new blood vessels in the diabetic wound via immunofluorescence staining. As shown in Figure 7(A), the expression of CD31 in the Exos-treated group was highest on day 7. It was also statistically determined that Exos significantly enhanced the expression of CD31 in a dose-dependent manner (Figure 7(B)). On the contrary, the combination of Exos and LPS significantly reduced the expression of CD31 when compared with the treatment of Exos alone. Being consistent with the

results we obtained above, Exos enhanced neovascularization at the wound sites of SD rats with type 1 diabetes.

Immunohistochemistry staining

To evaluate the degree of inflammation variation in diabetic wounds treated with PBS, Exos, and the combination of Exos and LPS, immunohistochemical (IHC) analysis was used to determine the levels of TNF- α and IL-6 as markers of inflammation in the diabetic wound tissues. According to Figure 8, a great deal of TNF- α and IL-6 staining, indicative of inflammation, were observed in the tissue sections treated with PBS. Moreover, Exos treatment substantially reduced the expression levels of TNF- α and IL-6 in the wound tissues. Meanwhile, when LPS as the activator of inflammation was combined with Exos to treat diabetic wound, local inflammation was significantly triggered by increasing the levels of IL-6 and TNF- α when compared with the treatment of Exos alone. All data proved that Exos exerted its anti-inflammatory effects as a direct result of the inhibition of pro-inflammatory enzymes and cytokines, such as IL-6 and TNF- α .

Western blot analysis in wound tissues

The effect of Exos on inflammatory inhibition and angiogenesis was further determined by western blot. According to Figure 9, Exos treatment significantly reduced the expression of TNF- α and IL-6 at the diabetic wound site as compared to that in PBS treated group. Furthermore, with the mediation of Exos and LPS as the activator of inflammation, levels of IL-6 and TNF- α also restored to be increased. To determine whether Exos could activate cell proliferation signaling pathways, western blotting was carried out to assess the protein levels of AKT and p-AKT in diabetic wound tissues following treatment with PBS, Exos, and the combination of Exos and LPS. The western blotting results revealed that Exos induced

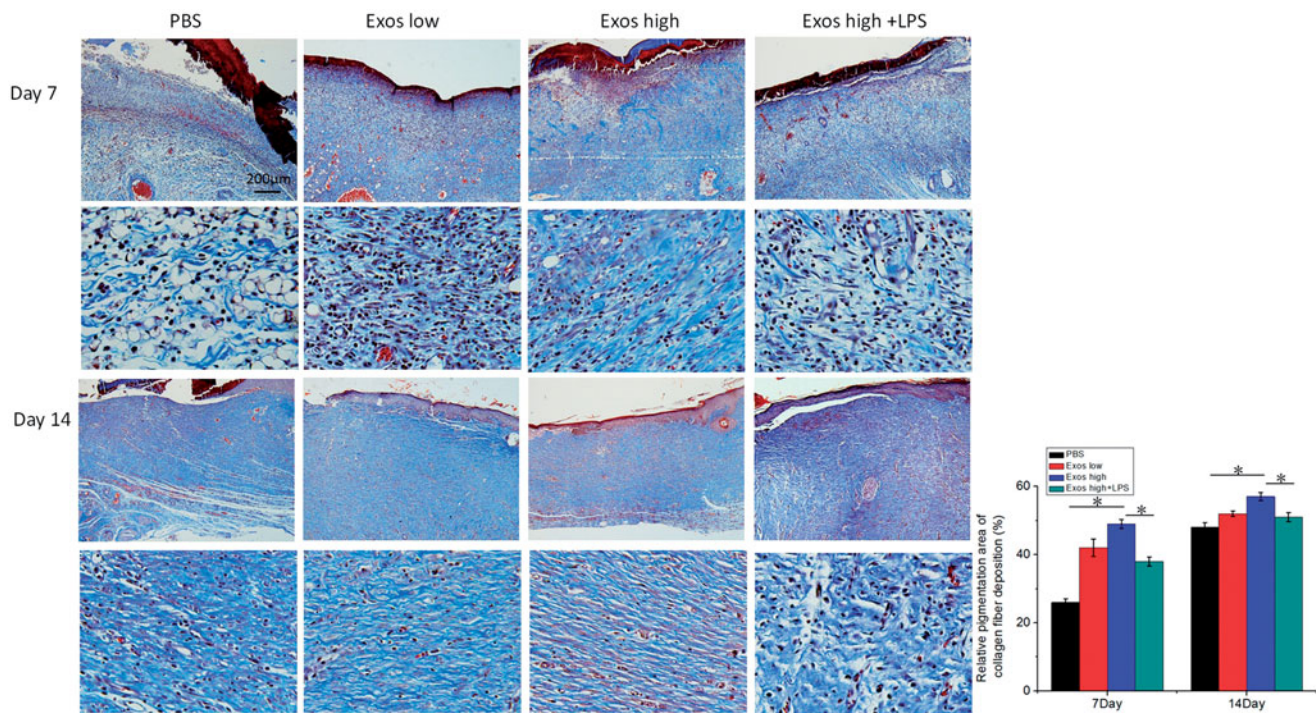


Figure 6. Masson's trichrome staining of wound sections treated with PBS, low Exos concentrations (100 µg/mL), high Exos concentrations (1 mg/mL), or high Exos (1 mg/mL) + LPS (10 µg/mL) concentrations at days 7 and 14. The data are presented as the means \pm SD ($n = 3$); $*p < .05$. The scale bar in all figure is 200 µm. The relative pigmentation area (%) was determined by calculating the ratio of area of the blue stain (collagen fibers) to the whole selected area.

significant increases in the phosphorylation of AKT (P-AKT), but LPS (as an inflammation activator) markedly reversed its upregulation of p-AKT induced by Exos. We also evaluated the protein level of MMP-9 and determined whether Exos could improve wound healing by inhibiting the expression of local MMP-9. The results indicated that when compared to the PBS group, Exos could effectively downregulate the expression levels of MMP-9 in the local diabetic wound, thus improving the pathophysiological status of diabetic wounds and accelerating the wound-healing process of diabetic rats.

Discussion

At present, many studies have reported that the process of diabetic wound healing was affected by intense and prolonged inflammation; thus, a treatment strategy preventing inflammation shows promising potential for promoting diabetic wound healing [27,28]. A previous study demonstrates that exosomes secreted by macrophage cells influenced inflammatory pathways and contributed to the resolution of inflammation in the recipient cells [29–31]. Therefore, in the present study, we assessed the possible mechanism of the anti-inflammatory effects of Exos for improving diabetic wound repair. Based on our results, we provided evidence that Exos improved the diabetic wound-healing effects mediated, at least in part, by the inhibition of the inflammatory signaling pathway. Exos obviously accelerated the diabetic wound healing rate and enhanced the quality of wound healing, as demonstrated by accelerated re-epithelialization, angiogenesis promotion, and the weakened infiltration of inflammatory cells. Meanwhile, Exos significantly inhibited the inflammatory response by decreasing the secretion of

TNF- α and IL-6 [32]. As vascular endothelial cells contributed to vascularization in a skin wound [33], we first focused on the biological response of vascular endothelial cells induced by Exos. When diabetic wound injury was occurred, vascular endothelial cells exposed to high glucose (HG) conditions, thus resulting in endothelial dysfunction characterized by significantly decreasing migration and proliferation as compared to that in normal glucose condition (control), impairing wound healing in patients with diabetes. Therefore, we employed high glucose cultured HUVECs (HG-HUVECs) to mimic diabetic environment *in vitro*. It was found that Exos played a positive role in promoting the angiogenic effects in HG-HUVECs. The western blot results also confirmed that Exos induced the inhibition of inflammation by reducing the production of TNF- α and IL-6. Secondly, we evaluated diabetic wound healing effects following treatment with Exos *in vivo*. In a full-thickness excisional diabetic wound model, Exos were subcutaneously injected into the diabetic wound site; we then investigated the neovascularization, re-epithelialization, and granulation tissue formation during the diabetic wound-healing process. It was found that Exos contributed to the wound-healing process by remarkably enhancing the wound size reduction. The infiltration of inflammatory cells in diabetic wounds was reduced and the granulation tissue that contained more congested blood vessels was rapidly formed, indicating that Exos induced inflammation inhibition and neo-angiogenesis. Masson's trichrome staining results showed that Exos boosted collagen deposition and re-epithelialization for accelerating wound healing.

In western blot experiments of wound tissues, we found that Exos effectively inhibited inflammatory signal transduction *in vivo* and revealed significant inhibitory effects by

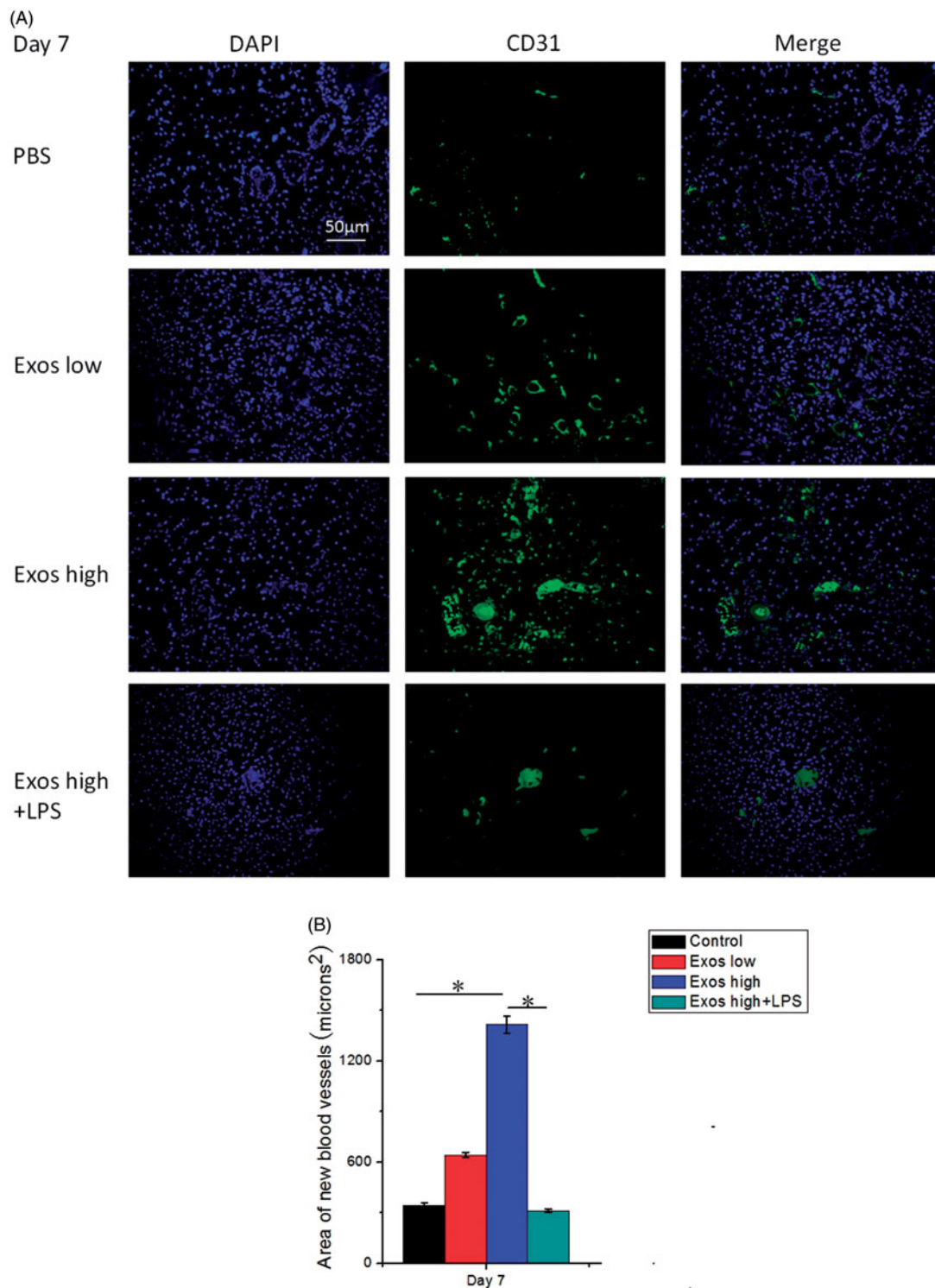


Figure 7. (A) Immunofluorescence staining of CD31. Newly formed blood vessels were identified by positive CD31 staining at postoperative day 7. The scale bar in figure 7 A is 50 μ m. (B) Quantitative analysis of the number of blood vessels. The data are represented as the means \pm SD ($n = 3$), $*p < .05$.

reducing the production of $\text{TNF-}\alpha$ and IL-6. Furthermore, the P-AKT was significantly activated and the MMP-9 level was sharply reduced following the injection of Exos, partly contributing to the faster wound-healing rate.

In order to further confirm our hypothesis that Exos-induced angiogenesis-promoting and proliferation effects were mediated by the inhibition of inflammation, we used LPS to stimulate the strong inflammatory response and

further investigated whether the variation of inflammation was related with Exos induced angiogenesis and LPS induced inflammation abolished the angiogenesis effects of Exos. It was found that in contrast with treatment of Exos alone, treatment with the combination of Exos and LPS significantly reversed the Exos induced angiogenesis-promoting effects and anti-inflammatory response, thus attenuating Exos-mediated wound-healing acceleration effects.

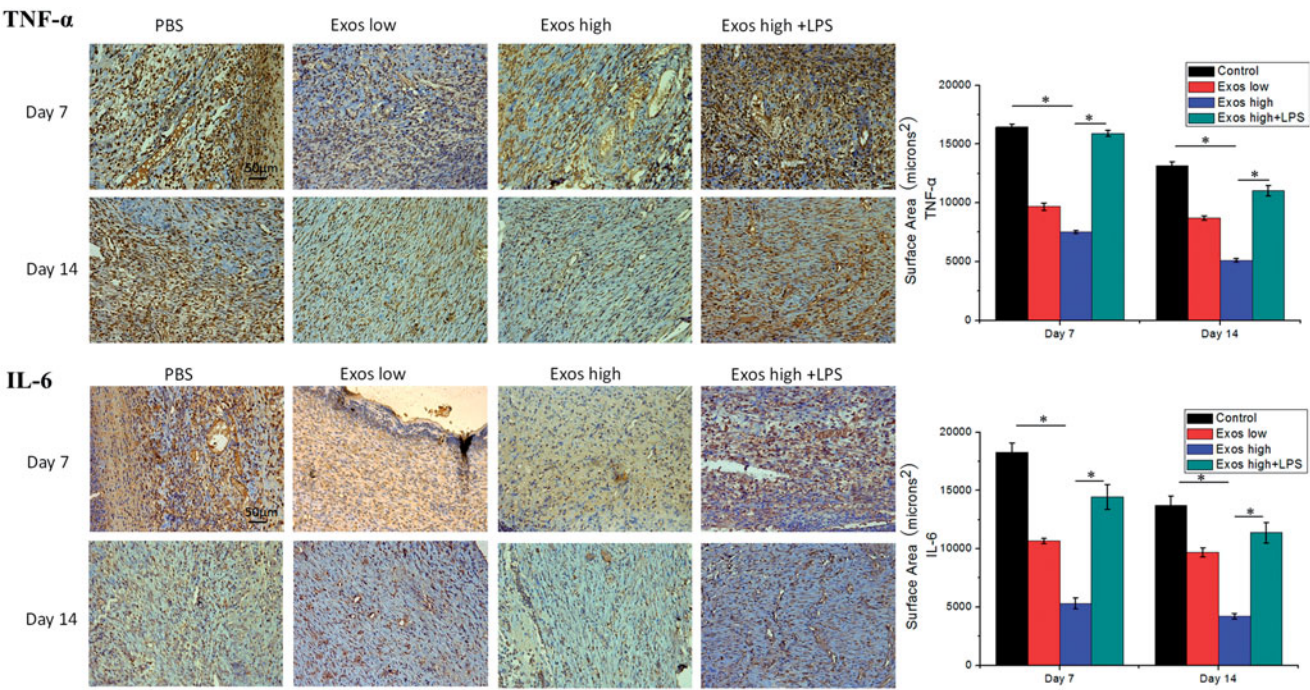


Figure 8. Immunohistochemistry analysis of IL-6 expression and TNF- α expression in diabetic wound sites treated with PBS, low concentrations of Exos, high concentrations of Exos, and high Exos + LPS concentrations at days 7 and 14; quantitative analysis of IL-6 expression and TNF- α expression. The data are presented as the means \pm SD ($n = 3$); $*p < .05$.

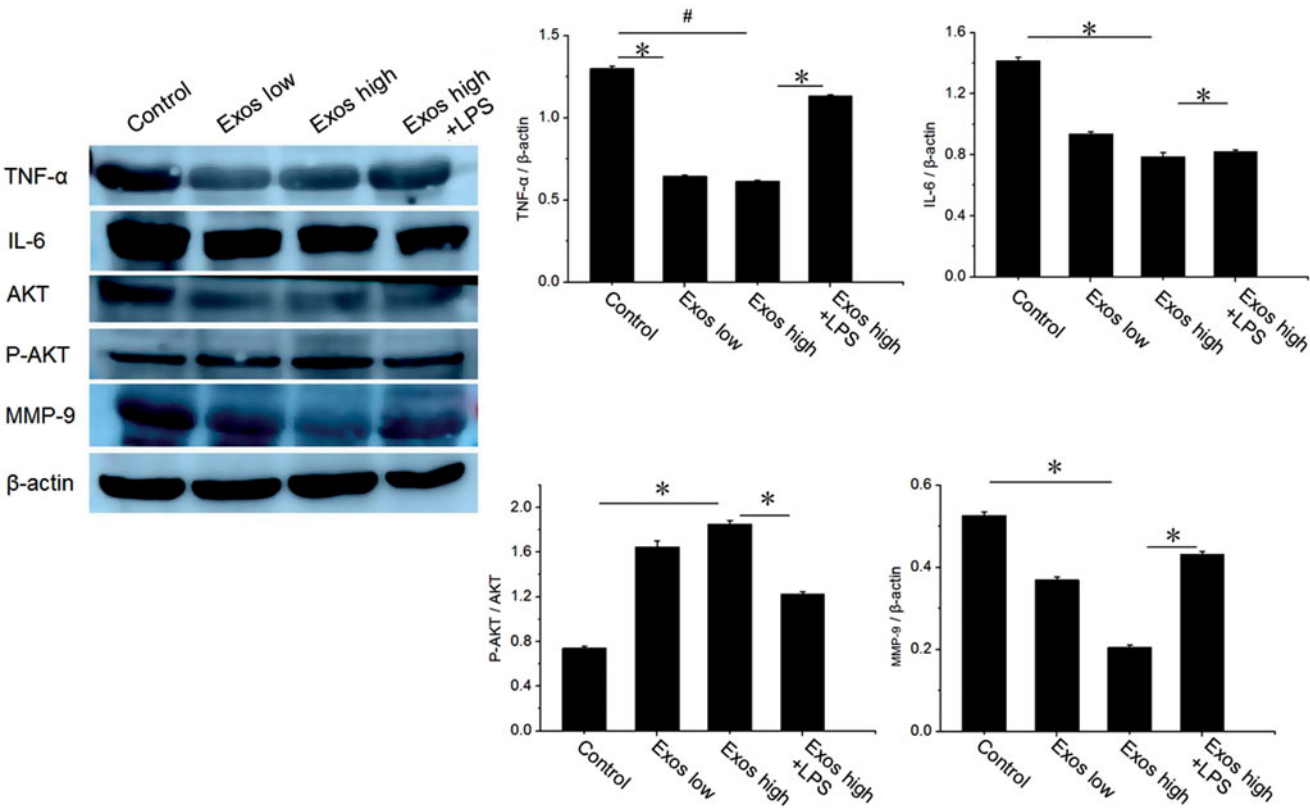


Figure 9. Detection of the levels of AKT, P-AKT, TNF- α , IL-6 and MMP-9 by Western blotting; the data are presented as the means \pm SD ($n = 3$); $\#p < .05$, compared PBS group with high Exos levels (1 mg/mL), $*p < .05$.

Conclusions

In summary, the present study confirmed that Exos exerted anti-inflammatory effects via inhibiting the secretion of proinflammatory enzymes and cytokines, and contributed to the

success of diabetic wound treatment by significantly accelerating angiogenesis and improving repair quality. Our findings suggest that exosomes derived from macrophage may represent a novel therapeutic strategy in the treatment of diabetic wound damage.

Disclosure statement

No potential conflict of interest was reported by the authors.

Funding

This work was supported by grants from the Scientific Research Project of Liaoning Provincial Department of Education [JYTQN201719] and Natural Science Foundation of Liaoning Province [No 20180550649]. We thank the above funders for their support. English-language editing of this manuscript was provided by Journal Prep Services.

References

- [1] Armstrong DG, Boulton AJM, Bus SA. Diabetic foot ulcers and their recurrence. *N Engl J Med*. 2017;376(24):2367–2375.
- [2] Meloni M, Izzo V, Giurato L, et al. Recurrence of critical limb ischemia after endovascular intervention in patients with diabetic foot ulcers. *Adv Wound Care (New Rochelle)*. 2018;7(6):171–176.
- [3] Avitabile S, Odorisio T, Madonna S, et al. Interleukin-22 promotes wound repair in diabetes by improving keratinocyte pro-healing functions. *J Invest Dermatol*. 2015;135(11):2862–2870.
- [4] Wang W, Yan X, Lin Y, et al. Wnt7a promotes wound healing by regulation of angiogenesis and inflammation: issues on diabetes and obesity. *J Dermatol Sci*. 2018;91(2):124.
- [5] Wang Y, Liu J, Kong Q, et al. Cardiomyocyte-specific deficiency of HSPB1 worsens cardiac dysfunction by activating NFκB-mediated leukocyte recruitment after myocardial infarction. *Cardiovasc Res*. 2018;115(1):154–167.
- [6] Nguyen TT, Ding D, Wolter WR, et al. Expression of active matrix metalloproteinase-9 as a likely contributor to the clinical failure of acclastide in treatment of diabetic foot ulcers. *Eur J Pharmacol*. 2018;834:77–83.
- [7] Wang W, Yang C, Wang XY, et al. MicroRNA-129 and -335 promote diabetic wound healing by inhibiting Sp1-mediated MMP-9 expression. *Diabetes*. 2018;67(8):1627–1638.
- [8] Zhuge Y, Regueiro MM, Tian R, et al. The effect of estrogen on diabetic wound healing is mediated through increasing the function of various bone marrow-derived progenitor cells. *J Vasc Surg*. 2018;68(6):1275.
- [9] Zhang B, Wang M, Gong A, et al. HucMSC-exosome mediated-Wnt4 signaling is required for cutaneous wound healing. *Stem Cells*. 2015;33(7):2158–2168.
- [10] El Andaloussi S, Mager I, Breakefield XO, et al. Extracellular vesicles: biology and emerging therapeutic opportunities. *Nat Rev Drug Discov*. 2013;12:347–357.
- [11] Johnsen KB, Gudbergsson JM, Skov MN, et al. A comprehensive overview of exosomes as drug delivery vehicles - endogenous nanocarriers for targeted cancer therapy. *Biochim Biophys Acta*. 2014;1846(1):75–87.
- [12] Lamichhane TN, Raiker RS, Jay SM. Exogenous DNA loading into extracellular vesicles via electroporation is size-dependent and enables limited gene delivery. *Mol Pharm*. 2015;12(10):3650–3657.
- [13] Guo S, Tao S, Yin W, et al. Exosomes derived from platelet-rich plasma promote the re-epithelization of chronic cutaneous wounds via activation of YAP in a diabetic rat model. *Theranostics*. 2017;7(1):81–96.
- [14] Hu Y, Rao S, Wang Z, et al. Exosomes from human umbilical cord blood accelerate cutaneous wound healing through miR-21-3p-mediated promotion of angiogenesis and fibroblast function. *Theranostics*. 2018;8(1):169–184.
- [15] Shi H, Xu X, Zhang B, et al. 3,3'-Diindolylmethane stimulates exosomal Wnt11 autocrine signaling in human umbilical cord mesenchymal stem cells to enhance wound healing. *Theranostics*. 2017;7(6):1674–1688.
- [16] Fang P, Li X, Dai J, et al. Immune cell subset differentiation and tissue inflammation. *J Hematol Oncol*. 2018;11(1):97.
- [17] Samblas M, Martínez JA, Milagro F. Folic acid improves the inflammatory response in LPS-activated THP-1 macrophages. *Mediators Inflamm*. 2018;2018:1312626.
- [18] Singhto N, Kanlaya R, Nilnumkhum A, et al. Roles of macrophage exosomes in immune response to calcium oxalate monohydrate crystals. *Front Immunol*. 2018;9:316.
- [19] Wang S, Xu M, Li X, et al. Exosomes released by hepatocarcinoma cells endow adipocytes with tumor-promoting properties. *J Hematol Oncol*. 2018;11(1):82.
- [20] Zhang D, Lee H, Wang X, et al. Exosome-mediated small RNA delivery: a novel therapeutic approach for inflammatory lung responses. *Mol Ther*. 2018;26(9):2119.
- [21] McDonald MK, Tian Y, Qureshi RA, et al. Functional significance of macrophage-derived exosomes in inflammation and pain. *Pain*. 2014;155(8):1527–1539.
- [22] Park JY, Shin MS, Hwang GS, et al. Beneficial effects of deoxyshikonin on delayed wound healing in diabetic mice. *IJMS*. 2018;19(11):3660.
- [23] Cai HA, Huang L, Zheng LJ, et al. Ginsenoside (Rg-1) promoted the wound closure of diabetic foot ulcer through iNOS elevation via miR-23a/IRF-1 axis. *Life Sci*. 2019;233:116525.
- [24] Nocera AL, Mueller SK, Stephan JR, et al. Exosome swarms eliminate airway pathogens and provide passive epithelial immunoprotection through nitric oxide. *J Allergy Clin Immunol*. 2018;143(4):1525.e1–1535.e1.
- [25] Li X, Yu M, Chen L, et al. LncRNA PMS2L2 protects ATDC5 chondrocytes against lipopolysaccharide-induced inflammatory injury by sponging miR-203. *Life Sci*. 2018;217:283–292.
- [26] Kong L, Wu Z, Zhao H, et al. Bioactive injectable hydrogels containing desferrioxamine and bioglass for diabetic wound healing. *ACS Appl Mater Interfaces*. 2018;10(36):30103–30114.
- [27] Frykberg RG, Banks J. Challenges in the treatment of chronic wounds. *Adv Wound Care (New Rochelle)*. 2015;4(9):560–582.
- [28] Xu Q, A S, Gao Y, et al. A hybrid injectable hydrogel from hyperbranched PEG macromer as a stem cell delivery and retention platform for diabetic wound healing. *Acta Biomaterialia*. 2018;75:63–74.
- [29] Squadrito ML, Baer C, Burdet F, et al. Endogenous RNAs modulate microRNA sorting to exosomes and transfer to acceptor cells. *Cell Rep*. 2014;8(5):1432–1446.
- [30] Kalani A, Tyagi A, Tyagi N. Exosomes: mediators of neurodegeneration, neuroprotection and therapeutics. *Mol Neurobiol*. 2014;49(1):590–600.
- [31] Recalcati S, Gammella E, Buratti P, et al. Macrophage ferroportin is essential for stromal cell proliferation in wound healing. *Haematologica*. 2018;104(1):47–58.
- [32] Wu Y, Qiu W, Xu X, et al. Exosomes derived from human umbilical cord mesenchymal stem cells alleviate inflammatory bowel disease in mice through ubiquitination. *Am J Transl Res*. 2018;10(7):2026–2036.
- [33] Driskell RR, Lichtenberger BM, Hoste E, et al. Distinct fibroblast lineages determine dermal architecture in skin development and repair. *Nature*. 2013;504(7479):277–281.